



First identification of late Mesozoic intraplate magmatism in the Chinese north Tianshan: implications for the orogenic architecture and crustal evolution

Fujun Wang^{1,2}, Zhiyuan He³, Rongfeng Ge¹, Meng Luo¹, Bihai Zheng¹, Zhiyong Zhang⁴, Rongsong Tian⁵, Yuanyuan Cao⁶ and Wenbin Zhu^{1*}

¹ State Key Laboratory for Mineral Deposits Research, Institute of Continental Geodynamics, School of Earth Sciences and Engineering, Nanjing University, Nanjing 210023, China

² Institute for Geosciences, University of Potsdam, 14469 Potsdam, Germany

³ Laboratory for Mineralogy and Petrology, Department of Geology, Ghent University, Krijgslaan 281 S8, 9000 Ghent, Belgium

⁴ State Key Laboratory of Lithospheric Evolution, Institute of Geology and Geophysics, Chinese Academy of Sciences, Beijing 100029, China

⁵ College of Resources and Environmental Engineering, Guizhou University, Guiyang 550025, China

⁶ School of Geography and Ocean Science, Nanjing University, Nanjing 210023, China

FW, 0000-0003-3474-4465; ZH, 0000-0002-5169-5557; RG, 0000-0001-5690-9289; ML, 0009-0000-5998-8533; BZ, 0000-0002-9766-8263; ZZ, 0000-0002-8841-8799; YC, 0009-0008-7310-7067; WZ, 0000-0002-2487-0161

*Correspondence: zwb@nju.edu.cn

Abstract: The formation and dynamics of granitoids in an intra-continental setting are crucial for understanding the architecture and evolution of continental crust. Here, we report geochronological, geochemical and Sr–Nd–Hf isotopic data for newly discovered late Mesozoic granitic intrusions in the Tianshan belt, northwestern China. These granitoids are I-type granites derived from an igneous precursor and were emplaced at c. 145–132 Ma. They have positive $\varepsilon_{\text{Na}}(t)$ values and young Nd model ages, together with relatively low Sr/Y ratios, indicating that they might have originated from partial melting of the juvenile lower crust. There is a prominent decoupling between zircon Hf and bulk-rock Nd isotopes, which may have resulted from the early crystallization of Ti-rich minerals. These granitic intrusions also display subduction-related geochemical characteristics, which are probably inherited from Paleozoic crustal sources that were metasomatized by subduction-related fluids. We conclude that these late Mesozoic granitoids were emplaced in an intra-continental setting, and were probably triggered by thermal relaxation owing to crustal shortening and thickening. These data further imply that the Tianshan changed into crustal reworking during the Mesozoic from its prominent crustal growth in the Paleozoic.

Supplementary material: LA-ICP-MS zircon U–Pb dating results, whole-rock major and trace element compositions, whole-rock Sr–Nd isotopic data and zircon Lu–Hf isotopic data are available at <https://doi.org/10.6084/m9.figshare.c.7167890>

Thematic collection: This article is part of the Mesozoic and Cenozoic tectonics, landscape and climate change collection available at: <https://www.lyellcollection.org/topic/collections/mesozoic-and-cenozoic-tectonics-landscape-and-climate-change>

Received 11 October 2023; revised 25 February 2024; accepted 14 March 2024

The Central Asian Orogenic Belt (CAOB), one of the largest accretionary orogens in the world, lies between the Tarim–North China cratons to the south and the East European and Siberian cratons to the north (Şengör *et al.* 1993; Jahn *et al.* 2000; Windley *et al.* 2007) (Fig. 1a). It is widely accepted that the ancestral CAOB was established during the Neoproterozoic–Paleozoic (Şengör *et al.* 1993; Xiao *et al.* 2009; Charvet *et al.* 2011), and parts of it were then reactivated in response to accretionary and collisional events along the Eurasian margin during the Mesozoic–Cenozoic (Hendrix *et al.* 1994; Jolivet *et al.* 2010). Situated in the southernmost part of the CAOB, the Tianshan orogenic belt connects to the Tarim Basin to the south and the Junggar Basin to the north (Fig. 1b). Over the last two decades, numerous investigations have been carried out on its Paleozoic accretionary (Windley *et al.* 2007; Xiao *et al.* 2009; Han *et al.* 2010) and subsequent early Mesozoic (i.e. Triassic) post-orogenic processes (Zhang *et al.* 2017; Liu *et al.* 2020; Feng and Zheng 2021). However, numerous uncertainties persist concerning the late Mesozoic (i.e. Jurassic–Cretaceous) magmatic and tectonic evolution of the Tianshan, primarily stemming from the absence of contemporaneous records of deformation and magmatism (Wang *et al.* 2022a).

It is generally accepted that there was no substantial magmatism in the late Mesozoic since the Palaeo-Asian Ocean finally closed during the late Paleozoic–Triassic (Xiao *et al.* 2009; Kröner *et al.* 2014; Tan *et al.* 2022). Despite this, recent detrital zircon geochronological data from clastic deposits in the SE Junggar Basin (Fig. 1b) showed the existence of abundant Jurassic–Cretaceous magmatic zircons (Yang 2013; Fang *et al.* 2015; Ji *et al.* 2018; Wang *et al.* 2022a). Provenance investigations further indicate that they were mainly sourced from the Tianshan in the south (Yang 2013; Wang *et al.* 2022a). In addition, a few late Mesozoic volcanic rock outcrops have also been documented from the Chinese North Tianshan (Wang and Gao 2012; Deng *et al.* 2015; Wang *et al.* 2022a). As a result, these lines of evidence point to the presence of late Mesozoic magmatism in the Tianshan. However, their origins and associated tectonism remain poorly investigated.

A late Mesozoic granitic intrusion was initially identified in the Bogda Mountain of the North Tianshan (the Donggou intrusive rocks) during recent 1:50 000 regional field mapping (Fig. 1c–e) (SRIGMR 2016). However, there has been a notable absence of research on its petrogenesis, magma source and tectonic implications. In this contribution, we first established a geochronological

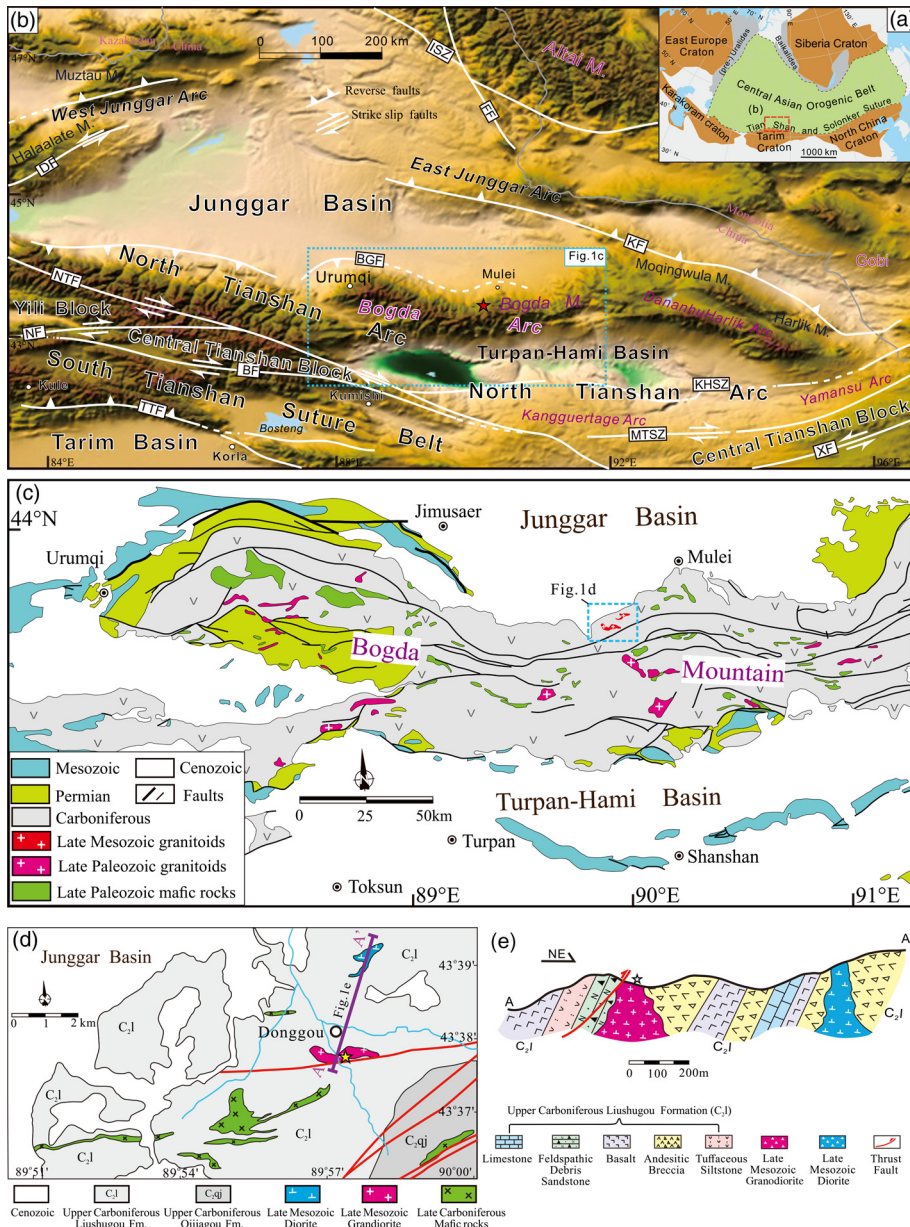


Fig. 1. (a) Tectonic framework of the Central Asian Orogenic Belt (CAOB) and surrounding regions. (b) Topographic map of the Chinese Tianshan belt. (c) Schematic geological map of the Bogda Mountain. (d) Geological map showing the locations of the late Mesozoic intrusive rocks. (e) Cross-section showing the contact relationship between the intrusions and the wall rock. Abbreviations: M., mountains; BF, Baluntai fault; BGF, Bogda fault; DF, Dalabute fault; FF, Fuyun fault; ISZ, Irtysh shear zone; KF, Kalamaili fault; KHSZ, Kangguer–Huangshan shear zone; MTSZ, Main Tianshan shear zone; NF, Nalati fault; NTF, North Tianshan fault; TTF, Tarim thrust fault. XF, Xingxingxia fault. Sources: (a) modified after Sengör *et al.* (1993); (c) modified after He *et al.* (2023); (d) SRIGMR (2016).

framework for these late Mesozoic igneous rocks using LA-ICP-MS zircon U-Pb dating. Then, their petrogenesis and tectonic context were determined using geochemical and Sr-Nd-Hf isotopic data. To examine the intra-continental crustal architecture and tectonic history of the late Mesozoic Tianshan, we finally integrated the available geochronological, geochemical and geophysical data in the area for a general discussion.

Geological setting and petrography

The Tianshan is a significant constituent of the southwestern Central Asian Orogenic Belt and extends from west to east through the Central Asian countries to the Xinjiang province in northwestern China (Windley *et al.* 2007; Xiao *et al.* 2008; Kröner *et al.* 2014). The Chinese segment of the Tianshan belt is located between the Tarim Basin to the south and the Junggar Basin to the north (Fig. 1b). It is traditionally subdivided into three tectonic units from north to south by ophiolite belts and major faults; namely, the North Tianshan Arc, the Yili–Central Tianshan Block and the South Tianshan Belt (Wang *et al.* 2007; Gao *et al.* 2008; Charvet *et al.* 2011) (Fig. 1b). It is also geographically divided into western and eastern segments by the Urumqi–Korla line (Xiao 2004) (Fig. 1b)

To the east of Urumqi, the North Tianshan is separated into two branches by the Turfan–Hami (Tu–Ha) Basin (Fig. 1b). The southern branch is in contact with the Central Tianshan along the Main Tianshan Zone and the northern one corresponds to the Bogda Arc, which is thrust onto the Junggar Basin toward the north and the Tu–Ha Basin toward the south (Charvet *et al.* 2011).

The Bogda Mountain encloses the northern part of the Chinese North Tianshan and is a ridge underlain by rocks of the Bogda Arc (Fig. 1b). It contains late Paleozoic to Quaternary sedimentary and igneous rocks (Fig. 1c) (Chen *et al.* 2011, 2013; Xie *et al.* 2016a, b, c). These strata generally underwent low-grade greenschist-facies metamorphism, and ductile thrusting locally occurred during the latest Permian–Triassic period (Chen *et al.* 2011, 2013; Xie *et al.* 2016a, b, c). The oldest sedimentary strata in the region are composed of Ordovician to Silurian marine clastic rocks and tuffs, interlayered with limestones and subordinate basalts (Chen *et al.* 2011, 2013; Xie *et al.* 2016a, b, c). The Devonian rocks in Bogda Mountain are dominated by marine–terrigenous tuffaceous sandstone and volcanic rocks (Chen *et al.* 2011, 2013; Xie *et al.* 2016a, b, c). The Carboniferous strata are in fault contact with the Devonian rocks and are divided into four formations; namely, the Lower Carboniferous Qijiaojing Formation (C_1qj) and the Upper

Carboniferous Liushugou Formation (C_2 l), Qijiagou Formation (C_{2qj}) and Aoeru Formation (C_{2ae}) (Chen *et al.* 2011, 2013; Xie *et al.* 2016a, b, c; Memtimin *et al.* 2020). These formations mainly consist of sandstone, mudstone, limestone, bioclastic limestone, tuff, basaltic rocks and andesite intercalated with rhyolite. Permian sediments unconformably overlie the Carboniferous rocks, and the sedimentary sequence progressively changes from marine to lacustrine, as observed at the NW margin of the Tuha basin. Lower Permian strata, consisting predominantly of marine turbidite sandstone and siliceous mudstone intercalated with bimodal lava, occur on the southern and northern flanks of the Bogda anticline. The Upper Permian consists of lacustrine siltstone and mudstone. Middle to Upper Permian thick red molasse is considered evidence for a post-orogenic setting. Triassic and Jurassic strata are dominated by conglomerates, sandstones and mudstones with coal-bearing successions (Tang *et al.* 2014).

The newly identified granitic intrusions have been found in the Donggou area of Mulei County and are tectonically located within the northern parts of the Bogda Arcs (Figs 1b and 2a). The granitic intrusions trend NW–SE (Fig. 1c and d) and the intrusive contact relationship between the intrusions and the country rocks is observed in the field (Fig. 2a–c). Specifically, an intrusive contact occurs at the north boundary between the intrusions and the andesitic breccia of the Late Carboniferous Liushugou Formation (C_2 l), whereas in the south boundary a fault contact exists between the intrusions and the feldspathic lithic sandstone of the Liushugou Formation (C_2 l) (Fig. 2b). Apparent fault scrapes can be recognized on the surface of both the feldspathic lithic sandstone and the granitic intrusions (Fig. 2c). Additionally, there is distinct zoning in the granularity of the Donggou intrusive rocks, with a gradual decrease in grain size from the core to the sides of the intrusion (Fig. 2d–f). Based on petrographic observations (Fig. 2g–l), the

Donggou granitoids predominantly consist of granodiorite and granodiorite porphyrite. The mineral assemblage of the granodiorite is predominantly composed of plagioclase (60%), alkali feldspar (15%), hornblende (10%), biotite (10%), quartz (5%), with minor paragenesis. The granodiorite porphyrite consists of phenocrysts (20%) and matrix (80%). The phenocrysts contain variable proportions of large plagioclase (15%) and hornblende (5%) grains with lengths from 0.7 to 2.4 cm. Of these, plagioclase is hypidiomorphic, with different extents of kaolinization, carbonatization and chloritization. Hornblende preserves a residual lamellar shape resulting from strong chloritization. The matrix is composed of plagioclase (50%), alkali feldspar (15%), quartz (10%) and hornblende (5%). Accessory minerals include zircon, magnetite and apatite.

Samples and analytical methods

Fresh and non-altered samples were collected along and perpendicular to the extension of the Donggou intrusive rocks. Three samples were chosen for LA-ICP-MS zircon U–Pb dating and Hf isotope analysis, 10 for whole-rock geochemistry and eight for whole-rock Sr–Nd isotope study. Supplementary material gives detailed analytical methods and protocols for geochronological, geochemical and isotopic analyses. The acquired data are presented in Supplementary material Tables S1–S4.

Results

Zircon U–Pb geochronology

The zircon U–Pb dating results for the three samples are listed in Supplementary material Table S1. The zircon grains exhibit



Fig. 2. Field and petrographic observations of the Donggou intrusive rocks in Bogda Mountain. (a) The granodiorite pluton; (b) intrusive relationship between the granodiorite and the surrounding strata; (c) fault striae on the surface of the granodiorite; (d–f) granodiorite with different grain sizes, with gradual coarsening of grain size from the sides of the intrusion towards the core; (g–j) coarse- to medium-grained granodiorite; (k–l) fine-grained granodiorite porphyrite. Abbreviations: Pl, plagioclase; Hb, hornblende; Qtz, quartz; Bt, biotite.

oscillatory zoning and lack inherited cores (Fig. 3) and high Th/U ratios, implying a magmatic origin. The data points from the fine-grained granodiorite porphyry (Sample DG20-15), the coarse- to medium-grained granodiorite (Sample DG20-8) and the coarse-

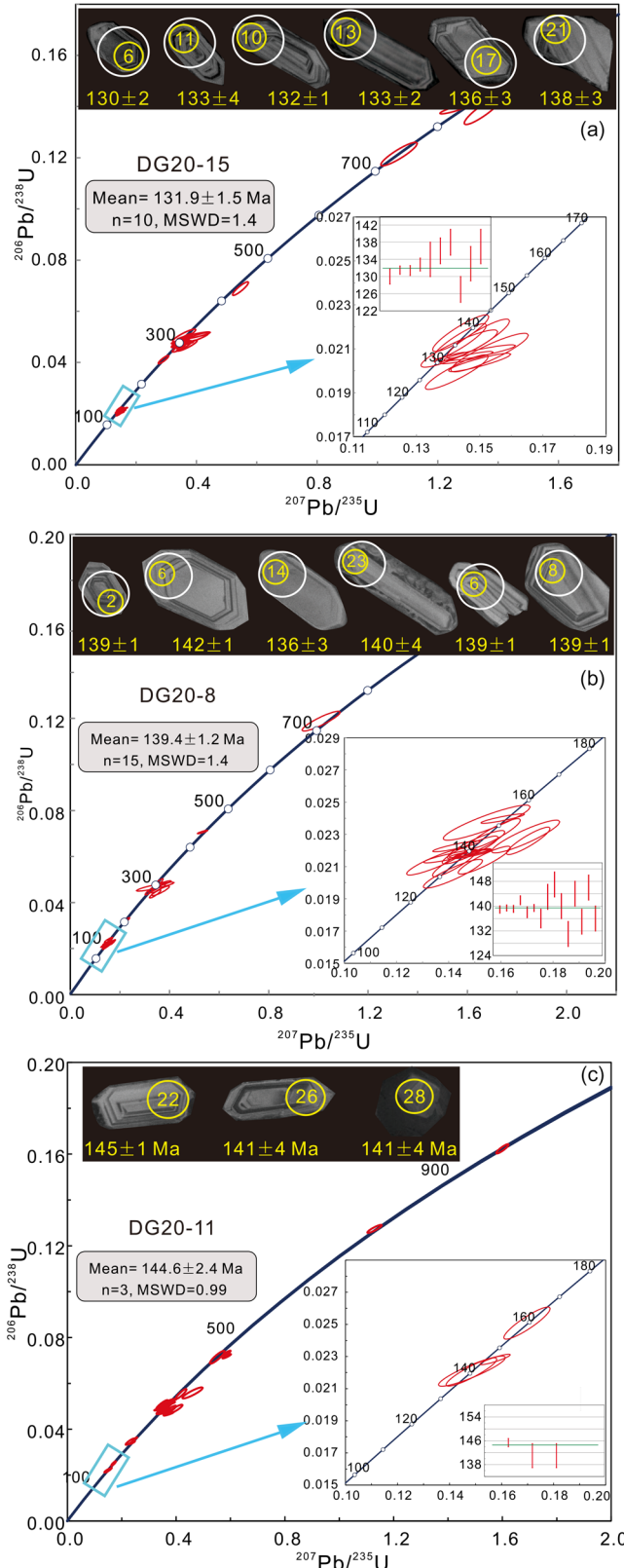


Fig. 3. Zircon U–Pb concordia diagrams and representative cathodoluminescence (CL) images for (a) granodiorite porphyry (sample DG20-15) and (b, c) granodiorite (samples DG20-8 and DG20-11) from the Donggou intrusive rocks. The yellow and white circles represent the sites of U–Pb dating and Hf isotope analysis, respectively.

grained granodiorite (Sample DG20-11) yielded weighted mean $^{206}\text{Pb}/^{238}\text{U}$ ages of 131.9 ± 1.5 Ma ($n = 10$; Fig. 3a), 139.4 ± 1.2 Ma ($n = 15$; Fig. 3b) and 144.6 ± 2.4 Ma ($n = 3$; Fig. 3c), respectively. Because the analysed zircon grains are of magmatic origin, these dates are interpreted as the time of zircon crystallization. These samples' weighted mean ages do not overlap within error, indicating that the Donggou granitic intrusions were probably emplaced in two periods roughly at 145–140 and 132 Ma, respectively.

Whole-rock major and trace elements

The major and trace element compositions are presented in Supplementary material Table S2 and plotted in Figure 4. The samples collected from the Donggou intrusive rocks exhibit high contents of SiO_2 (65.25–67.13 wt%), Al_2O_3 (14.46–15.16 wt%) and total-alkali ($\text{K}_2\text{O} + \text{Na}_2\text{O} = 6.77$ –8.54 wt%), with low contents of MgO (1.05–1.38 wt%), TiO_2 (0.66–0.74 wt%), P_2O_5 (0.15–0.19 wt%) and MnO (0.07–0.19 wt%) (Table S2). These samples also exhibit calc-alkaline to high-K calc-alkaline features (Fig. 4a) and metaluminous to weakly peraluminous properties (Fig. 4b), with aluminium saturation index ($\text{ASI} = \text{molar Al}_2\text{O}_3/(\text{CaO} + \text{Na}_2\text{O} + \text{K}_2\text{O})$) values between 0.9 and 1.0. Moreover, they have low $\text{Mg}^\#$ values (24.8–29.2), where $\text{Mg}^\# = 100 * (\text{MgO}/40)/(\text{MgO}/40 + \text{FeO}^\text{T}/72)$.

These samples show similar REE patterns (Fig. 4c), including enrichment of light rare earth elements (LREE), depletion of heavy rare earth elements (HREE) and mild negative Eu anomalies ($\delta\text{Eu} = 0.66$ –0.75), as shown on the chondrite-normalized REE diagram. These samples also display low (La/Yb)_N ratios (2.8–3.3), which show a lack of distinction between LREE and HREE. On the primitive mantle-normalized multi-element diagram (Fig. 4d), all the samples are enriched in large ion lithophile elements (LILE; Rb, Ba, Th and U) and depleted in high field strength elements (HFSE; Nb, Ta and Ti).

Whole-rock Sr–Nd and zircon Hf isotopes

The Sr and Nd isotopic compositions of representative samples are listed in Table S3 and shown in Figure 5a and b. The initial isotopic ratios were calculated using zircon U–Pb ages. The initial $^{87}\text{Sr}/^{86}\text{Sr}$ ratios for the Donggou intrusions are uniform ($I_{\text{Sr}} = 0.7051$ –0.7062), and positive $\varepsilon_{\text{Nd}}(t)$ values range from +5.5 to +5.8. The corresponding two-stage Nd model ages are *c.* 453–479 Ma. Table S4 and Figure 5c show *in situ* zircon Hf isotopic analyses for two samples of the late Mesozoic granodiorite. All analyses were performed on grains or domains of magmatic zircon that had oscillatory zoning. Fifteen Hf isotopic analyses for samples DG20-15 (*c.* 131.9 Ma) and DG20-8 (*c.* 139.4 Ma) have negative $\varepsilon_{\text{Hf}}(t)$ values between −14.2 to −9.5 and two-stage Hf model ages of *c.* 1763 to *c.* 2049 Ma.

Discussion

Distribution of late Mesozoic magmatic rocks

Figure 6 illustrates the spatial distribution of published geochronological data on late Mesozoic intrusive and volcanic rocks in the Tianshan and its adjacent regions. For example, near the Honggou section in the Manas River valley (southern Junggar Basin), thin tuff layers have been reported in the lower part of the Upper Jurassic Qigu Formation, and the dated zircons yielded crystallization ages between 165 and 157 Ma (Wang and Gao 2012; Deng *et al.* 2015). Similarly, a thin tuff layer has been documented in the lower part of the Qigu Formation at the Wangjiagou section near Urumqi, within the southern Junggar Basin, providing a weighted mean zircon $^{206}\text{Pb}/^{238}\text{U}$ age of 156 Ma (Wang *et al.* 2022a). In addition, some researchers have reported the presence of tuffs in the Upper Jurassic

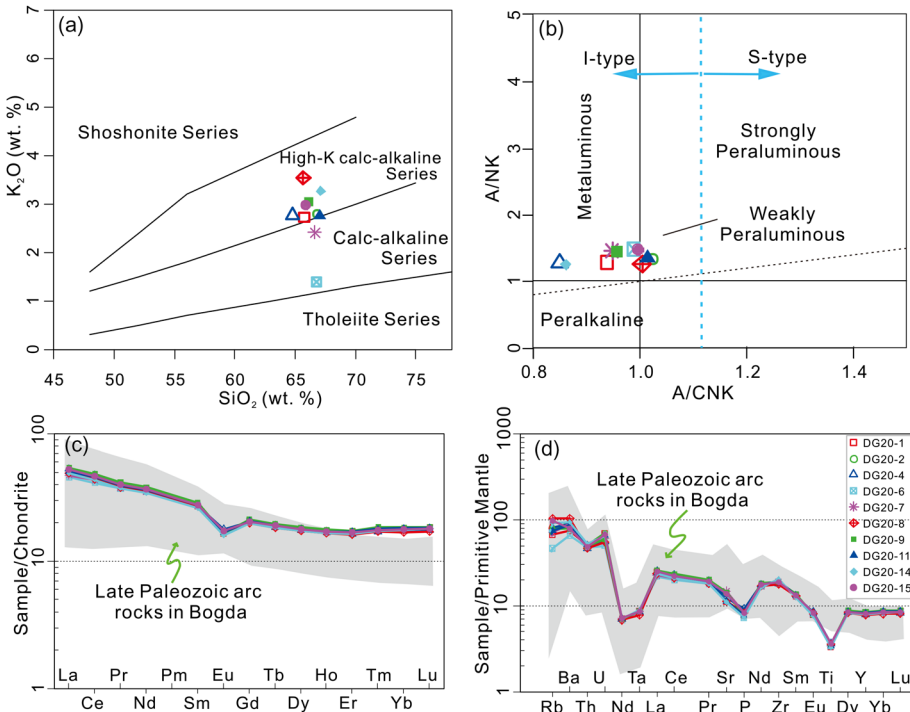


Fig. 4. Whole-rock (**a, b**) major and (**c, d**) trace element diagrams for the studied granitoid samples from the Donggou intrusive rocks. (**a**) K_2O v. SiO_2 diagram. (**b**) A/NK v. A/CNK diagram. (**c**) Chondrite-normalized REE pattern. (**d**) Primitive mantle-normalized trace element spider diagram. Sources: (a) Peccerillo and Taylor (1976); (b) Maniar and Piccoli (1989). (d) Values of chondrite and primitive mantle are from Boynton (1984) and Sun and McDonough (1989), respectively. Data for the late Paleozoic arc-related magmatic rocks in the Bogda Mountain are from Chen *et al.* (2011, 2013), Xie *et al.* (2016a, b, c), Memtimin *et al.* (2020) and Li *et al.* (2021).

Shishugou Formation in the Kalamaili and Bogda Mountains (Hendrix *et al.* 2001). Furthermore, utilizing the whole-rock $^{40}Ar/^{39}Ar$ method, researchers have obtained ages of 193 and 120–110 Ma for basalt in the Karamay region of the West Junggar Basin (Xu *et al.* 2008) and the Tuoyun region of the South Tianshan (Sobel and Arnaud 2000), respectively. Recent discoveries by Liu *et al.* (2018) include several Early Jurassic trachyandesites in the Fuyun region of the Altai Mountain, with a zircon $^{206}Pb/^{238}U$ age of 182 Ma. These findings provide robust evidence of late Mesozoic volcanic activity in the Tianshan and the Junggar Basin's margins. Meanwhile, some researchers have identified Late Jurassic granites in the Altai Mountain and Chinese North Tianshan, with zircon $^{206}Pb/^{238}U$ ages of 151 Ma (Wang *et al.* 2014) and 155–153 Ma (Liu *et al.* 2019), respectively. This further provides evidence for Jurassic intrusive magmatic activities in the Tianshan and Altai Mountains.

In this study, zircon U–Pb dating of the Donggou granitoids produced ages of 131.9 ± 1.5 , 139.4 ± 1.2 and 144.6 ± 2.4 Ma (Fig. 3). This marks the first identification of Early Cretaceous intrusive magmatism within the Chinese Tianshan region. Interestingly, a prior study had established an emplacement age of *c.* 154.9 Ma for the Donggou granitic intrusion, utilizing the LA-ICP-MS zircon U–Pb dating method (Liu *et al.* 2019). Given the discernible distinctions within the analytical uncertainties of these ages, our interpretation suggests that the emplacement of the Donggou intrusive rocks probably occurred in multiple stages. These stages encompass the Late Jurassic period at *c.* 155 Ma, followed by two subsequent stages in the Early Cretaceous period around 145–140 and 132 Ma, respectively.

Origin of the Donggou granitoids

The late Mesozoic Donggou granitoids exhibit relatively low incompatible element contents, low $FeO^T/(FeO^T + MgO)$ ratios and low $10\,000 \times Ga/Al$ ratios, indicating that they are not typical A-type granites. In the granite discrimination diagrams (Supplementary material Fig. S1a and b), these samples consistently plot within the I- or S-type field. They are characterized as metaluminous to slightly peraluminous, as evidenced by ASI values below 1.0, in contrast to strongly peraluminous S-type granites with

ASI values exceeding 1.1 (Chappell 1999). The negative correlation between P_2O_5 and SiO_2 appears to follow the I-type trend (Supplementary material Fig. S1c), which is an effective method for discriminating I- from S-type granites (Chappell and White 1992). Furthermore, in the Na_2O v. K_2O diagram (Supplementary material Fig. S1d), all samples fit within the I-type granite field. These characteristics indicate that the Donggou granitoids are calc-alkaline to high-K calc-alkaline I-type granites with high SiO_2 and low MgO contents. These characteristics, including considerable enrichment of LILE and depletion of HFSE (Fig. 4d), hint that the partial melting of crustal rocks could have played a role in forming the Donggou granitoids.

Relatively K-rich mafic to intermediate igneous rocks in the lower crust have been proposed as potential sources for such granitoids (Sisson *et al.* 2005). The compositional variation among the granitoid samples is elucidated through a discernible positive correlation in the $(La/Yb)N$ v. La diagram (see Supplementary material Fig. S1e), reinforcing the notion that these differences primarily arise from partial melting processes. We propose that the Donggou granitoids probably resulted from dehydration melting within the middle and lower crust, where the pronouncedly low porosity of metamorphic rocks restricts substantial water involvement (Du *et al.* 2018). Hydrous minerals, specifically amphibole and mica, are pivotal contributors to granitic magma generation through dehydration-melting (Borg and Clyne 1998). Notably, the examined samples exhibit relatively low K, Rb and Cs contents and low K_2O/Na_2O and Rb/Sr ratios (Supplementary material Table S2), which argue against the presence of mica in the source rocks. Moreover, the absence of concave-upward middle REE (MREE) to HREE patterns (see Fig. 4c) contradicts the notion of amphibole as a dominant residual phase, aligning with the expectations of amphibole dehydration-melting (Borg and Clyne 1998). Additionally, all samples project into the plagioclase stability area in the Sr/Y v. La/Yb diagram (Supplementary material Fig. S1f), indicating substantial plagioclase but no garnet in the residue during partial melting and therefore a melting pressure <8 kbar (Rapp and Watson 1995; Wang *et al.* 2016). Taking into account the low $(Ho/Yb)_N (<1)$, $Sr/Y (<9)$ and $La/Yb (<5)$ ratios, we hypothesize that the parental melts of the Donggou granitoids were probably formed by

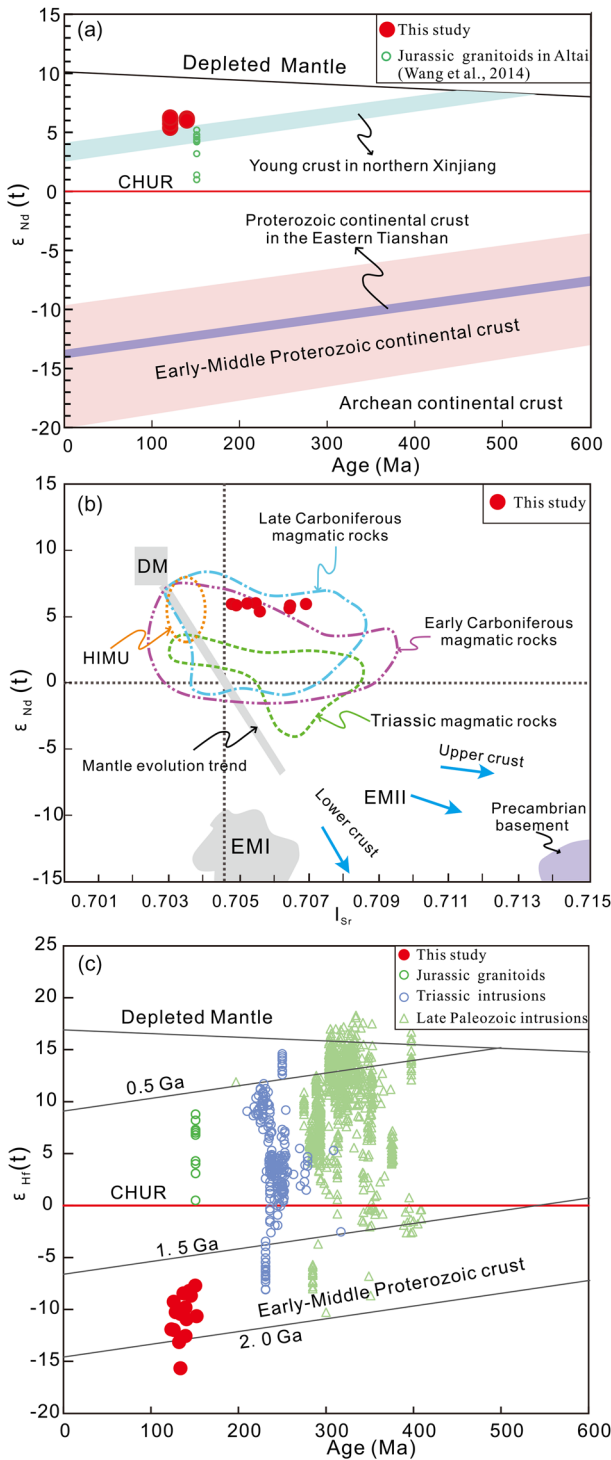


Fig. 5. (a) $\epsilon_{\text{Nd}}(t)$ - t diagram, (b) $\epsilon_{\text{Nd}}(t)$ - I_{Sr} diagram and (c) zircon $\epsilon_{\text{Hf}}(t)$ - t diagrams for the studied granitoid samples from the Donggou granitoids in the Bogda Mountain. Abbreviations: DM, depleted mantle; HIMU, high U/Pb mantle end element; EMI, enriched mantle (pelagic sediments); EMII, enriched mantle (terrigenous sediments). Sources: the Proterozoic continental crustal evolution line is from Jahn et al. (2000) and Jahn (2004), the juvenile crustal evolution line in northern Xinjiang is from Han et al. (1999), the Nd isotope data of the Late Jurassic granitoids in Altai Mountain are from Wang et al. (2014). Data for the Triassic granitoids in the eastern Tianshan are from Feng and Zheng (2021), data for the Early Carboniferous and Late Carboniferous mafic to felsic rocks in the Eastern Tianshan are from Hou et al. (2014), Jiang et al. (2017), Du et al. (2018) and Zhao et al. (2019), data for the Precambrian crust in the CAOB are from Kovalenko et al. (2004), zircon Hf isotope data for Late Jurassic granitoids in the Altai are from Wang et al. (2014), zircon Hf isotope data and sources for Late Paleozoic and Triassic intrusive rocks in the East Tianshan area are from Feng and Zheng (2021).

dehydration melting of amphibole-bearing mafic rocks in the lower to middle crust at relatively low pressure.

Nd–Hf isotopic decoupling constraints

The Donggou granitoids show high I_{Sr} values and positive $\epsilon_{\text{Nd}}(t)$ values (+5.5 to +5.8) with relatively young Nd model ages (*c.* 453–479 Ma) (Fig. 5a; Supplementary material Table S3), indicating a minimal contribution of ancient crust in magmatic evolution. On the t - $\epsilon_{\text{Nd}}(t)$ diagram (Fig. 5b), all samples fall close to the evolution array of juvenile crust in northern Xinjiang. This suggests that they were possibly derived from juvenile lower crust. Indeed, the geochemical (Fig. 4c and d) and Nd isotopic features (Fig. 5a) of the Donggou granitoids are similar to those of the Paleozoic bimodal volcanic rocks in the Bogda Mountain (Chen et al. 2011, 2013; Xie et al. 2016a, b, c; Memtimin et al. 2020). This similarity lends support to the model proposing the remelting of Paleozoic basaltic rocks as the source material.

In contrast to the positive $\epsilon_{\text{Nd}}(t)$ values and young Nd model ages discussed above, our zircon Hf isotopic data (Fig. 5c; Table S4) reveal that the Donggou granitoids have predominantly negative $\epsilon_{\text{Hf}}(t)$ values (-14.2 to -9.5) and old Hf model ages (1763–2049 Ma), suggesting a prominent decoupling between zircon Hf and bulk-rock Nd isotopes. Several hypotheses have been proposed for decoupled Nd–Hf isotopic compositions in granitic rocks, including the following: (1) enrichment of Lu and other HREE in garnet residues (Vervoort and Patchett 1996); (2) melting of a metasedimentary source with a high Lu/Hf ratio owing to ‘zircon effect’ (Patchett et al. 1984); (3) post-emplacement (metamorphic) disturbance of the Sm–Nd isotopic system in REE-bearing accessory mineral phases (e.g. apatite, allanite and titanite) (Hammerli et al. 2019); (4) partial melting of lithospheric mantle or juvenile lower crust with decoupled Nd–Hf isotopic compositions (Yu et al. 2017); (5) influence on Hf isotopic compositions from early formed Ti-rich minerals (Huang et al. 2019).

First, the Donggou granitoid samples show low La/Yb ratios (Supplementary material Fig. S1), suggesting plagioclase as a prominent remaining phase during partial melting rather than garnet. Second, the Donggou granitoids are I-type granites formed primarily by remelting of juvenile basaltic rocks in the lower crust, distinct from S-type granites derived from metasedimentary sources. Third, metamorphic disruption can also be ruled out because the Donggou granitoids do not exhibit considerable metamorphism. According to the fourth hypothesis, Nd–Hf isotope decoupling can be inherited from magma sources that experienced interactions between fluids (with high Nd/Hf ratios from subducting sediments or oceanic crust) and lithospheric mantle (Hanyu et al. 2006; Chauvel et al. 2009). This mechanism, however, would generate melts with high $\epsilon_{\text{Hf}}(t)$ and low $\epsilon_{\text{Nd}}(t)$ values, in contrast to Donggou granitoid samples’ high $\epsilon_{\text{Nd}}(t)$ and low $\epsilon_{\text{Hf}}(t)$ values. As a result, the fourth hypothesis is likewise unsuitable for the formation of the Donggou granitoids. The fifth hypothesis linked Nd–Hf isotopic decoupling to Ti-rich material crystallization (Huang et al. 2019). It is proposed that the early formed Ti-rich minerals (e.g. ilmenite, amphibole) are probably major Hf hosts and that they may record different Hf isotopes compared with the later-formed zircons (Huang et al. 2019). Hence, the early formed Ti-rich minerals will result in a difference in Nd–Hf isotopic compositions between the parental magma and zircons crystallized from the developed melt (Huang et al. 2019). The Donggou granitoids are rich in minerals such as amphibole, which are high in titanium. We hypothesize that the decoupling between bulk-rock Nd and zircon Hf isotopes may have been a result of the occurrence of these early formed Ti-rich minerals.

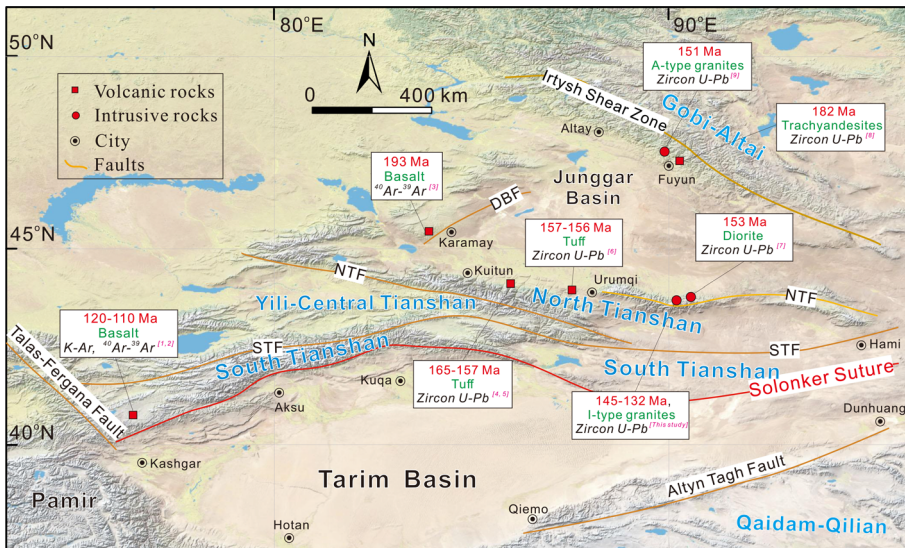


Fig. 6. Distribution of late Mesozoic magmatic rocks in the Tianshan and its adjacent areas. NTF, North Tianshan fault; STF, South Tianshan fault; DBF, Dalabute fault. Sources: [1] Sobel and Arnaud (2000); [2] Ji *et al.* (2006); [3] Xu *et al.* (2008); [4] Wang and Gao (2012); [5] Deng *et al.* (2015); [6] Wang *et al.* (2022a); [7] Liu *et al.* (2019); [8] Liu *et al.* (2018); [9] Wang *et al.* (2014).

Tectonic and crustal architecture significance

It is widely accepted that the majority of I-type granites typically form within subduction zones or in post-orogenic extensional settings, where the influx of volatiles and heat triggers partial melting of the deep-seated orogenic roots, ultimately giving rise to granitic magmas (Shellnutt *et al.* 2021). Also, the studied late Mesozoic Donggou granitoids exhibit typical subduction-related geochemical features (Supplementary material Fig. S2). However, previous researchers have concluded that the entire Eastern Tianshan, including the Bogda Mountain, has been in an intra-continental tectonic setting since the Triassic period (Du *et al.* 2018; Feng and Zheng 2021; Li *et al.* 2021). Further, numerous studies have demonstrated that the Tianshan (including the Bogda Mountain) was in a compressional tectonic setting during the Late Jurassic to earliest Cretaceous (*c.* 145 Ma), based on structural (Yang *et al.* 2015; Zhu *et al.* 2020; Wang *et al.* 2022a) and low-temperature thermochronological evidence (Tang *et al.* 2015; Gillespie *et al.* 2017; He *et al.* 2022, 2023; Luo *et al.* 2023). Therefore, the Donggou granitoids in the Bogda Mountain may have originated in an intra-continental compressional environment. The subduction-related geochemical characteristics were probably inherited from Paleozoic crustal sources metasomatized by subduction-related fluids (Zhang *et al.* 2017).

An alternative explanation points to the delamination of the continental lower crust induced by crustal thickening as a plausible mechanism for the generation of the Donggou I-type granites in such a tectonic regime (Fig. 7; Zhang *et al.* 2006). According to theories describing the stabilization of Andean arcs into a continental structure, it is likely that thermal relaxation, stemming

from the processes of crustal shortening and thickening, played a significant role in triggering Late Cretaceous intraplate magmatism within the Bogda Mountain (DeCelles *et al.* 2009; Ducea *et al.* 2015). Specifically, this thermal relaxation resulted in the upwelling of the asthenosphere beneath the Donggou region (Fig. 7). Consequently, the middle and lower crustal layers could have experienced underplating and intraplating by mantle-derived magmas owing to heating of the lithospheric mantle. This process, in turn, led to the partial melting of crustal rocks, ultimately producing the Donggou granitoid magmas (Fig. 7). This mechanism stands in stark contrast to the formation of the Late Jurassic Jiangjunshan A-type granites in the Altai Mountain (Fig. 7), which are believed to have originated from a mixed source composed of juvenile mantle-derived materials and a minor contribution from an older crustal source (Wang *et al.* 2014).

According to previous studies, the majority of Phanerozoic granitoids in the CAOB are characterized by positive $\varepsilon_{\text{Nd}}(t)$ values and young Nd model ages, suggesting that juvenile crust or depleted mantle contributed to the formation of these rocks (Jahn *et al.* 2000; Kovalenko *et al.* 2001, 2004; Jahn 2004). In the North Tianshan, the Nd isotopic compositions of the late Mesozoic granitoids are similar to those of the Paleozoic syn- and post-orogenic granitoids (Fig. 5). This implies that the basement of this terrane has maintained its original continental character (*i.e.* no new crustal growth). Some researchers have suggested that the CAOB represents the most critical region of crustal growth during the Phanerozoic (Jahn *et al.* 2000; Jahn 2004; Wang *et al.* 2022b, 2023). The evolution of the CAOB involved both lateral and vertical accretion of juvenile material, whereas the emplacement of large volumes of post-collisional granitoids was more probably accomplished by vertical

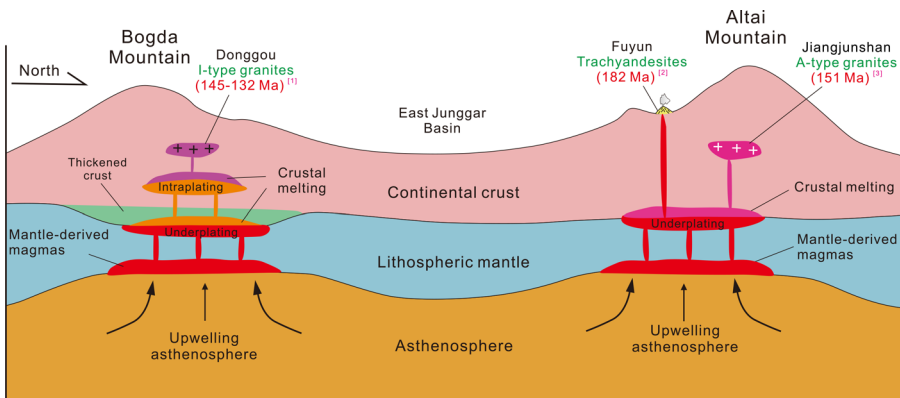


Fig. 7. Schematic diagram showing the generation of the Donggou I-type granites in the Bogda Mountain, and comparing with the formation of Jiangjunshan A-type granites in the Altai Mountain. The thickness of continental crust and lithospheric mantle are not to scale. Sources: the model is based on ideas from Ducea *et al.* (2015), Feng and Zheng (2021), Wang *et al.* (2022a) and Yuan *et al.* (2023). Sources of dating data: [1] this study; [2] Liu *et al.* (2018); [3] Wang *et al.* (2014).

crustal growth (Jahn 2004; Wang *et al.* 2022b). In contrast, other researchers have disagreed with this opinion and underlined the significance of recycling or remelting of older crustal material in the CAOB rather than the production of mantle-derived or juvenile crust in terms of Paleozoic granitoid generation (Kröner *et al.* 2014; Yu *et al.* 2017). Regardless, the geochemical and isotopic characteristics strongly indicate that the Mesozoic granites in the Tianshan belt were predominantly sourced from recycled crustal components, retaining the elemental and isotopic signatures of their protoliths (Zhao *et al.* 2019; Feng and Zheng 2021; Yuan *et al.* 2023). These data further imply that the Tianshan orogen underwent crustal reworking based on its initial architecture of Paleozoic crustal growth during the Mesozoic era. Our findings underscore that thermal relaxation driven by crustal shortening and thickening may have played an important role in generating small-scale intraplate crustal magmatism, leading to further differentiation and stabilization of continental crust in juvenile orogens.

A model has been put forth suggesting that the late Mesozoic crustal shortening and thickening in Tianshan and its adjacent areas resulted from strike-slip deformation induced by the differential rotation of blocks (Yin *et al.* 2023; Wang *et al.* 2024) (Supplementary material Fig. S3), such as the Junggar (Gilder *et al.* 2008; Choulet *et al.* 2012, 2013) and Tarim basins (Gilder *et al.* 2003, 2008). The rotation of these basins was accommodated by strike-slip faults in the Altai (e.g. the Irtysh shear zone), the Tianshan (e.g. the North Tianshan Fault) and the southeastern margin of the Tarim (e.g. the Xingxingxia and the Altn Tagh faults) (Wang *et al.* 2024). The spatial distribution of the late Mesozoic magmatism primarily occurred along the boundary of the Junggar and Tarim basins (Fig. 6), which also supports this hypothesis. Furthermore, this rotation of blocks can be linked to several far-distant tectonic processes in the Central Asian highlands (Zhu *et al.* 2020; Wang *et al.* 2022a, 2024) (Supplementary material Fig. S3), including (1) accretion of the Kolyma–Omolon Block to the Siberian Craton (Oxman 2003), (2) closure of the Mongol–Okhotsk Ocean (Yang *et al.* 2015), (3) collision of the Karakoram–Lhasa Block with Eurasia (Yang *et al.* 2017) and (4) the subduction of the Meso-Tethys oceanic plate (Kapp *et al.* 2007).

Conclusions

- (1) The Donggou granitoids were emplaced between c. 145 and c. 132 Ma, demonstrating, for the first time, that Early Cretaceous magmatic activity occurred in the North Tianshan.
- (2) These intrusions might have originated from partial melting of the Paleozoic juvenile crust, further stressing the late Mesozoic crustal reworking in the Tianshan.
- (3) Decoupling between zircon Hf and bulk-rock Nd isotopes is probably due to the early crystallization of Ti-rich crystals.
- (4) The Donggou granitoids were formed in an intra-continental setting, possibly dynamically linked to thermal relaxation driven by crustal shortening and thickening.

Scientific editing by Renjie Zhou

Acknowledgements We thank two anonymous reviewers for detailed and constructive comments, and associate editor Renjie Zhou for editorial handling.

Author contributions FW: conceptualization (lead), data curation (lead), investigation (lead), methodology (lead), writing – original draft (lead), writing – review & editing (lead); ZH: conceptualization (equal), supervision (lead), writing – review & editing (equal); RG: conceptualization (equal), methodology (equal), supervision (lead), writing – review & editing (equal);

ML: conceptualization (equal), data curation (equal), investigation (equal), writing – review & editing (supporting); BZ: conceptualization (equal), data curation (equal), resources (equal), writing – review & editing (supporting); ZZ: data curation (supporting), formal analysis (equal), methodology (lead), writing – review & editing (supporting); RT: methodology (supporting), software (lead), validation (equal), writing – review & editing (supporting); YC: investigation (equal), writing – review & editing (supporting); WZ: conceptualization (lead), funding acquisition (lead), investigation (lead), project administration (lead), supervision (lead), writing – review & editing (lead)

Funding This work was funded by the National Natural Science Foundation of China (Grant no. 92162211), and funding by the China Scholarship Council (no. 202206190029) financed the research stay of F. J. Wang in Germany.

Competing interests The authors declare that they have no known competing financial interests or personal relationships that could have appeared to influence the work reported in this paper.

Data availability All data generated in this study are available in the supplementary information files.

References

- Borg, L.E. and Clyne, M.A. 1998. The petrogenesis of felsic calc-alkaline magmas from the Southernmost Cascades, California: origin by partial melting of basaltic lower crust. *Journal of Petrology*, **39**, 1197–1222, <https://doi.org/10.1093/petro/39.6.1197>
- Boynton, W.V. 1984. Cosmochemistry of the rare earth elements: meteorite studies. In: P. Henderson (ed.) *Rare Earth Element Geochemistry*. Elsevier, **2**, 63–114, <https://doi.org/10.1016/b978-0-444-42148-7.50008-3>
- Chappell, B.W. 1999. Aluminium saturation in I- and S-type granites and the characterization of fractionated haplogranites. *Lithos*, **46**, 535–551, [https://doi.org/10.1016/s0024-4937\(98\)00086-3](https://doi.org/10.1016/s0024-4937(98)00086-3)
- Chappell, B.W. and White, A.J.R. 1992. I- and S-type granites in the Lachlan Fold Belt. *Earth and Environmental Science Transactions of the Royal Society of Edinburgh*, **83**, 1–26, <https://doi.org/10.1017/s0263593300007720>
- Charvet, J., Shu, L. *et al.* 2011. Palaeozoic tectonic evolution of the Tianshan belt, NW China. *Science China Earth Sciences*, **54**, 166–184, <https://doi.org/10.1007/s11430-010-4138-1>
- Chauvel, C., Marini, J., Plank, T. and Ludden, J.N. 2009. Hf–Nd input flux in the Izu–Mariana subduction zone and recycling of subducted material in the mantle. *Geochemistry, Geophysics, Geosystems*, **10**, <https://doi.org/10.1029/2008gc002101>
- Chen, X., Shu, L. and Santosh, M. 2011. Late Paleozoic post-collisional magmatism in the Eastern Tianshan Belt, Northwest China: new insights from geochemistry, geochronology and petrology of bimodal volcanic rocks. *Lithos*, **127**, 581–598, <https://doi.org/10.1016/j.lithos.2011.06.008>
- Chen, X., Shu, L., Santosh, M. and Zhao, X. 2013. Island arc-type bimodal magmatism in the eastern Tianshan Belt, Northwest China: geochemistry, zircon U–Pb geochronology and implications for the Paleozoic crustal evolution in Central Asia. *Lithos*, **168**, 48–66, <https://doi.org/10.1016/j.lithos.2012.10.006>
- Choulet, F., Faure, M., Cluzel, D., Chen, Y., Lin, W. and Wang, B. 2012. From oblique accretion to transpression in the evolution of the Altai collage: new insights from West Junggar, northwestern China. *Gondwana Research*, **21**, 530–547, <https://doi.org/10.1016/j.gr.2011.07.015>
- Choulet, F., Chen, Y. *et al.* 2013. First Triassic palaeomagnetic constraints from Junggar (NW China) and their implications for the Mesozoic tectonics in Central Asia. *Journal of Asian Earth Sciences*, **78**, 371–394, <https://doi.org/10.1016/j.jseas.2013.01.023>
- DeCelles, P.G., Ducea, M.N., Kapp, P. and Zandt, G. 2009. Cyclicity in Cordilleran orogenic systems. *Nature Geoscience*, **2**, 251–257, <https://doi.org/10.1038/ngeo469>
- Deng, S., Wang, S., Yang, Z., Lu, Y. and Wan, X. 2015. Comprehensive study of the Middle–Upper Jurassic Strata in the Junggar Basin, Xinjiang. *Acta Geoscientica Sinica*, **36**, 559–574 [in Chinese with English abstract].
- Du, L., Long, X., Yuan, C., Zhang, Y., Huang, Z., Wang, X. and Yang, Y. 2018. Mantle contribution and tectonic transition in the Aqishan–Yamansu Belt, Eastern Tianshan, NW China: insights from geochronology and geochemistry of Early Carboniferous to Early Permian felsic intrusions. *Lithos*, **304**, 230–244, <https://doi.org/10.1016/j.lithos.2018.02.010>
- Ducea, M.N., Saleeby, J.B. and Bergantz, G. 2015. The architecture, chemistry, and evolution of continental magmatic arcs. *Annual Review of Earth and Planetary Sciences*, **43**, 1–33, <https://doi.org/10.1146/annurev-earth-060614-105049>
- Fang, Y., Wu, C., Guo, Z., Hou, K., Dong, L., Wang, L. and Li, L. 2015. Provenance of the southern Junggar Basin in the Jurassic: evidence from detrital zircon geochronology and depositional environments. *Sedimentary Geology*, **315**, 47–63, <https://doi.org/10.1016/j.sedgeo.2014.10.014>

- Feng, W. and Zheng, J. 2021. Triassic magmatism and tectonic setting of the eastern Tianshan, NW China: constraints from the Weiya intrusive complex. *Lithos*, **394**, 106171, <https://doi.org/10.1016/j.lithos.2021.106171>
- Gao, J., Long, L. et al. 2008. Tectonic evolution of the South Tianshan orogen and adjacent regions, NW China: geochemical and age constraints of granitoid rocks. *International Journal of Earth Sciences*, **98**, 1221, <https://doi.org/10.1007/s00531-008-0370-8>
- Gilder, S., Chen, Y., Cogné, J.-P., Tan, X., Courtillot, V., Sun, D. and Li, Y. 2003. Paleomagnetism of Upper Jurassic to Lower Cretaceous volcanic and sedimentary rocks from the western Tarim Basin and implications for inclination shallowing and absolute dating of the M-0 (ISEA?) chron. *Earth and Planetary Science Letters*, **206**, 587–600, [https://doi.org/10.1016/s0012-821x\(02\)01074-9](https://doi.org/10.1016/s0012-821x(02)01074-9)
- Gilder, S.A., Gomez, J., Chen, Y. and Cogné, J. 2008. A new paleogeographic configuration of the Eurasian landmass resolves a paleomagnetic paradox of the Tarim Basin (China). *Tectonics*, **27**, <https://doi.org/10.1029/2007tc002155>
- Gillespie, J., Glorie, S., Jepson, G., Zhang, Z.Y., Xiao, W.J., Danišík, M. and Collins, A.S. 2017. Differential exhumation and crustal tilting in the Easternmost Tianshan (Xinjiang, China), revealed by low-temperature thermochronology. *Tectonics*, **36**, 2142–2158, <https://doi.org/10.1002/2017tc004574>
- Hammerli, J., Kemp, A.I.S. and Whitehouse, M.J. 2019. In situ trace element and Sm–Nd isotope analysis of accessory minerals in an Eoarchean tonalitic gneiss from Greenland: implications for Hf and Nd isotope decoupling in Earth's ancient rocks. *Chemical Geology*, **524**, 394–405, <https://doi.org/10.1016/j.chemgeo.2019.06.025>
- Han, B., He, G. and Wang, S. 1999. Postcollisional mantle-derived magmatism, underplating and implications for basement of the Junggar Basin. *Science in China Series D: Earth Sciences*, **42**, 113–119, <https://doi.org/10.1007/bf02878509>
- Han, B.-F., Guo, Z.-J., Zhang, Z.-C., Zhang, L., Chen, J.-F. and Song, B. 2010. Age, geochemistry, and tectonic implications of a late Paleozoic stitching pluton in the North Tian Shan suture zone, western China. *Geological Society of America Bulletin*, **122**, 627–640, <https://doi.org/10.1130/b26491.1>
- Hanyu, T., Tatsumi, Y. et al. 2006. Contribution of slab melting and slab dehydration to magmatism in the NE Japan arc for the last 25 Myr: constraints from geochemistry. *Geochemistry, Geophysics, Geosystems*, **7**, <https://doi.org/10.1029/2005gc001220>
- He, Z., Wang, B. et al. 2022. Mesozoic building of the Eastern Tianshan and East Junggar (NW China) revealed by low-temperature thermochronology. *Gondwana Research*, **103**, 37–53, <https://doi.org/10.1016/j.gr.2021.11.013>
- He, Z., Glorie, S. et al. 2023. A re-evaluation of the Meso-Cenozoic thermo-tectonic evolution of Bogda Shan (Tian Shan, NW China) based on new basement and detrital apatite fission track thermochronology. *International Geology Review*, **65**, 2093–2112, <https://doi.org/10.1080/00206814.2022.121946>
- Hendrix, M.S., Dumitru, T.A. and Graham, S.A. 1994. Late Oligocene–early Miocene unroofing in the Chinese Tian Shan: an early effect of the India–Asia collision. *Geology*, **22**, 487–490, [https://doi.org/10.1130/0091-7613\(1994\)022<0487:LOEMUI>2.3.CO;2](https://doi.org/10.1130/0091-7613(1994)022<0487:LOEMUI>2.3.CO;2)
- Hendrix, M.S., Graham, S.A., Carroll, A.R., Sobel, E.R., McKnight, C.L., Schulein, B.J. and Wang, Z.X. 2001. Sedimentary record and climatic implications of recurrent deformation in the Tian Shan: evidence from Mesozoic strata of the north Tarim, south Junggar, and Turpan basins, northwest China. *Geological Society of America Bulletin*, **113**, 53–79, [https://doi.org/10.1130/0016-7606\(1992\)104<0053:sracio>2.3.co;2](https://doi.org/10.1130/0016-7606(1992)104<0053:sracio>2.3.co;2)
- Hou, T., Zhang, Z., Santos, M., Encarnacion, J., Zhu, J. and Luo, W. 2014. Geochronology and geochemistry of submarine volcanic rocks in the Yamansu iron deposit, Eastern Tianshan Mountains, NW China: constraints on the metallogenesis. *Ore Geology Reviews*, **56**, 487–502, <https://doi.org/10.1016/j.oregeorev.2013.03.008>
- Huang, H., Niu, Y., Teng, F.-Z. and Wang, S.-J. 2019. Discrepancy between bulk-rock and zircon Hf isotopes accompanying Nd–Hf isotope decoupling. *Geochimica et Cosmochimica Acta*, **259**, 17–36, <https://doi.org/10.1016/j.gca.2019.05.031>
- Jahn, B.-M. 2004. The Central Asian Orogenic Belt and growth of the continental crust in the Phanerozoic. *Geological Society, London, Special Publications*, **226**, 73–100, <https://doi.org/10.1144/gsl.sp.2004.226.01.05>
- Jahn, B., Wu, F. and Chen, B. 2000. Massive granitoid generation in Central Asia: Nd isotope evidence and implication for continental growth in the Phanerozoic. *Episodes*, **23**, 82–92, <https://doi.org/10.18814/epiugs/2000/v23i2/001>
- Ji, H., Tao, H., Wang, Q., Qiu, Z., Ma, D., Qiu, J. and Liao, P. 2018. Early to Middle Jurassic tectonic evolution of the Bogda Mountains, Northwest China: evidence from sedimentology and detrital zircon geochronology. *Journal of Asian Earth Sciences*, **153**, 57–74, <https://doi.org/10.1016/j.jseas.2017.03.018>
- Ji, J., Han, B., Zhu, M., Chu, Z. and Liu, Y. 2006. Cretaceous–Paleogene alkaline magmatism in Tuyun basin, southwest Tianshan mountains: geochronology, petrology and geochemistry. *Acta Petrologica Sinica*, **5**, 1324–1340 [in Chinese with English abstract].
- Jiang, H., Han, J., Chen, H., Zheng, Y., Lu, W., Deng, G. and Tan, Z. 2017. Intracontinental back-arc basin inversion and Late Carboniferous magmatism in Eastern Tianshan, NW China: constraints from the Shaquanzi magmatic suite. *Geoscience Frontiers*, **8**, 1447–1467, <https://doi.org/10.1016/j.gsf.2017.01.008>
- Jolivet, M., Dominguez, S., Charreau, J., Chen, Y., Li, Y. and Wang, Q. 2010. Mesozoic and Cenozoic tectonic history of the central Chinese Tian Shan: reactivated tectonic structures and active deformation. *Tectonics*, **29**, <https://doi.org/10.1029/2010tc002712>
- Kapp, P., DeCelles, P.G., Gehrels, G.E., Heizler, M. and Ding, L. 2007. Geological records of the Lhasa–Qiangtang and Indo-Asian collisions in the Nima area of central Tibet. *Geological Society of America Bulletin*, **119**, 917–933, <https://doi.org/10.1130/b26033.1>
- Kovalenko, V.I., Yarmolyuk, V.V. et al. 2001. Isotope structure of crust and mantle in the Central Asia Mobile Belt: geochronological and isotopic (Nd, Sr and Pb) data. *Gondwana Research*, **4**, 668–669, [https://doi.org/10.1016/s1342-937x\(05\)70464-0](https://doi.org/10.1016/s1342-937x(05)70464-0)
- Kovalenko, V.I., Yarmolyuk, V.V., Kovach, V.P., Kotov, A.B., Kozakov, I.K., Salnikova, E.B. and Larin, A.M. 2004. Isotope provinces, mechanisms of generation and sources of the continental crust in the Central Asian mobile belt: geological and isotopic evidence. *Journal of Asian Earth Sciences*, **23**, 605–627, [https://doi.org/10.1016/s1367-9120\(03\)00130-5](https://doi.org/10.1016/s1367-9120(03)00130-5)
- Kröner, A., Kovach, V. et al. 2014. Reassessment of continental growth during the accretionary history of the Central Asian Orogenic Belt. *Gondwana Research*, **25**, 103–125, <https://doi.org/10.1016/j.gr.2012.12.023>
- Li, D., He, D., Lu, Y., Fan, D., Zhen, Y. and Hou, S. 2021. Diverse origins of late Paleozoic calc-alkaline magmatic rocks from the Bogda tectonic belt: implications for the geodynamic evolution of the eastern Tianshan, NW China. *Lithos*, **404**, 106442, <https://doi.org/10.1016/j.lithos.2021.106442>
- Liu, S., Dou, H., Zhang, W., Peng, Z., Zhang, L. and Zhang, W. 2018. Discovery of Jurassic trachyanandesite and its geological significance in the northwestern of Junggar Basin. *Geological Review*, **64**, 1519–1529 [in Chinese with English abstract].
- Liu, S., Dou, H., Li, H. and Wen, Z. 2019. Geological significance of the discovery of Late Jurassic intermediate-acidic intrusive rock in Bogeda area of East Tianshan, Xinjiang, and its U-Pb zircon age. *Geological Bulletin of China*, **38**, 288–294 [in Chinese with English abstract].
- Liu, S., Wang, R. et al. 2020. Indosinian magmatism and rare metal mineralization in East Tianshan orogenic belt: an example study of Jing'erqun Li–Be–Nb–Ta pegmatite deposit. *Ore Geology Reviews*, **116**, 103265, <https://doi.org/10.1016/j.oregeorev.2019.103265>
- Luo, M., He, Z. et al. 2023. Exhumation and preservation of the Tianyu Cu–Ni deposit constrained by low-temperature thermochronology: insights into the thermo-tectonic history of the Chinese Eastern Tianshan. *Ore Geology Reviews*, **154**, 105309, <https://doi.org/10.1016/j.oregeorev.2023.105309>
- Maniar, P.D. and Piccoli, P.M. 1989. Tectonic discrimination of granitoids. *Geological Society of America Bulletin*, **101**, 635–643, [https://doi.org/10.1130/0016-7606\(1989\)101<0635:TDOG>2.3.CO;2](https://doi.org/10.1130/0016-7606(1989)101<0635:TDOG>2.3.CO;2)
- Memtimin, M., Pe-Piper, G., Piper, D.J.W., Guo, Z. and Zhang, Y. 2020. Carboniferous arc-related volcanism in SW Bogda Mountain, Northwest China, and its implications for regional tectonics. *Lithos*, **360**, 105413, <https://doi.org/10.1016/j.lithos.2020.105413>
- Oxman, V.S. 2003. Tectonic evolution of the Mesozoic Verkhoyansk–Kolyma belt (NE Asia). *Tectonophysics*, **365**, 45–76, [https://doi.org/10.1016/s0040-1951\(03\)00064-7](https://doi.org/10.1016/s0040-1951(03)00064-7)
- Patchett, P.J., White, W.M., Feldmann, H., Kielinczuk, S. and Hofmann, A.W. 1984. Hafnium/rare earth element fractionation in the sedimentary system and crustal recycling into the Earth's mantle. *Earth and Planetary Science Letters*, **69**, 365–378, [https://doi.org/10.1016/0012-821x\(84\)90195-x](https://doi.org/10.1016/0012-821x(84)90195-x)
- Peccerillo, A. and Taylor, S.R. 1976. Geochemistry of Eocene calc-alkaline volcanic rocks from the Kastamonu area, Northern Turkey. *Contributions to Mineralogy and Petrology*, **58**, 63–81, <https://doi.org/10.1007/bf00384745>
- Rapp, R.P. and Watson, E.B. 1995. Dehydration melting of metabasalt at 8–32 kbar: implications for continental growth and crust–mantle recycling. *Journal of Petrology*, **36**, 891–931, <https://doi.org/10.1093/petrology/36.4.891>
- Sengör, A.M.C., Natal'ín, B.A. and Burtman, V.S. 1993. Evolution of the Altai tectonic collage and Palaeozoic crustal growth in Eurasia. *Nature*, **364**, 299–307, <https://doi.org/10.1038/364299a0>
- Shellnutt, J.G., Denysyn, S.W. and Pang, K.-N. 2021. Editorial: granite petrogenesis and geodynamics. *Frontiers in Earth Science*, **8**, 637729, <https://doi.org/10.3389/feart.2020.637729>
- Sisson, T.W., Ratajeski, K., Hankins, W.B. and Glazner, A.F. 2005. Voluminous granitic magmas from common basaltic sources. *Contributions to Mineralogy and Petrology*, **148**, 635–661, <https://doi.org/10.1007/s00410-004-0632-9>
- Sobel, E.R. and Arnaud, N. 2000. Cretaceous–Paleogene basaltic rocks of the Tuyun basin, NW China and the Kyrgyz Tian Shan: the trace of a small plume. *Lithos*, **50**, 191–215, [https://doi.org/10.1016/s0024-4937\(99\)00046-8](https://doi.org/10.1016/s0024-4937(99)00046-8)
- SRIGMR 2016. *Regional Geological Map of Keenkaleng Sheet (K45E003024)*, scale 1:50,000. Shaanxi Regional Institute of Geology and Mineral Resources.
- Sun, S.-S. and McDonough, W.F. 1989. Chemical and isotopic systematics of oceanic basalts: implications for mantle composition and processes. *Geological Society, London, Special Publications*, **42**, 313–345, <https://doi.org/10.1144/gsl.sp.1989.042.01.19>
- Tan, Z., Xiao, W. et al. 2022. Final closure of the Paleo Asian Ocean basin in the early Triassic. *Communications Earth & Environment*, **3**, 259, <https://doi.org/10.1038/s43247-022-00578-4>
- Tang, W., Zhang, Z., Li, J., Li, K., Chen, Y. and Guo, Z. 2014. Late Paleozoic to Jurassic tectonic evolution of the Bogda area (northwest China): evidence from detrital zircon U–Pb geochronology. *Tectonophysics*, **626**, 144–156, <https://doi.org/10.1016/j.tecto.2014.04.005>
- Tang, W., Zhang, Z., Li, J., Li, K., Luo, Z. and Chen, Y. 2015. Mesozoic and Cenozoic uplift and exhumation of the Bogda Mountain, NW China: evidence

- from apatite fission track analysis. *Geoscience Frontiers*, **6**, 617–625, <https://doi.org/10.1016/j.gsf.2014.04.006>
- Vervoort, J.D. and Patchett, P.J. 1996. Behavior of hafnium and neodymium isotopes in the crust: constraints from Precambrian crustally derived granites. *Geochimica et Cosmochimica Acta*, **60**, 3717–3733, [https://doi.org/10.1016/0016-7037\(96\)00201-3](https://doi.org/10.1016/0016-7037(96)00201-3)
- Wang, B., Chen, Y. *et al.* 2007. Primary Carboniferous and Permian paleomagnetic results from the Yili Block (NW China) and their implications on the geodynamic evolution of Chinese Tianshan Belt. *Earth and Planetary Science Letters*, **263**, 288–308, <https://doi.org/10.1016/j.epsl.2007.08.037>
- Wang, F., Luo, M., He, Z., Ge, R., Cao, Y., Grave, J.D. and Zhu, W. 2022a. Late Mesozoic intracontinental deformation and magmatism in the Chinese Tianshan and adjacent areas, Central Asia. *Geological Society of America Bulletin*, **134**, 3003–3021, <https://doi.org/10.1130/b36318.1>
- Wang, F., Luo, M. *et al.* 2024. Mid-Cretaceous accelerated cooling of the Beishan Orogen, NW China: evidence from Apatite Fission Track Thermochronology. *Lithosphere*, **2023**, https://doi.org/10.2113/2023/lithosphere_2023_239
- Wang, Q., Hawkesworth, C.J. *et al.* 2016. Pliocene–Quaternary crustal melting in central and northern Tibet and insights into crustal flow. *Nature Communications*, **7**, 11888, <https://doi.org/10.1038/ncomms11888>
- Wang, S. and Gao, L. 2012. SHRIMP U–Pb dating of zircons from tuff of Jurassic Qigu Formation in Junggar Basin, Xinjiang. *Geological Bulletin of China*, **31**, 503–509 [in Chinese with English abstract].
- Wang, T., Jahn, B.-M. *et al.* 2014. Mesozoic intraplate granitic magmatism in the Altai accretionary orogen, NW China: implications for the orogenic architecture and crustal growth. *American Journal of Science*, **314**, 1–42, <https://doi.org/10.2475/01.2014.01>
- Wang, T., Huang, H. *et al.* 2022b. Voluminous continental growth of the Altaiids and its control on metallogeny. *National Science Review*, **10**, nwac283, <https://doi.org/10.1093/nsr/nwac283>
- Wang, T., Xiao, W.J. *et al.* 2023. Quantitative characterization of orogens through isotopic mapping. *Communications Earth & Environment*, **4**, 110, <https://doi.org/10.1038/s43247-023-00779-5>
- Windley, B.F., Alexeiev, D., Xiao, W., Kröner, A. and Badarch, G. 2007. Tectonic models for accretion of the Central Asian Orogenic Belt. *Journal of the Geological Society, London*, **164**, 31–47, <https://doi.org/10.1144/0016-76492006-022>
- Xiao, W., Han, C. *et al.* 2008. Middle Cambrian to Permian subduction-related accretionary orogenesis of Northern Xinjiang, NW China: implications for the tectonic evolution of central Asia. *Journal of Asian Earth Sciences*, **32**, 102–117, <https://doi.org/10.1016/j.jseas.2007.10.008>
- Xiao, W.-J. 2004. Paleozoic accretionary and collisional tectonics of the eastern Tianshan (China): implications for the continental growth of central Asia. *American Journal of Science*, **304**, 370–395, <https://doi.org/10.2475/ajs.304.4.370>
- Xiao, W.J., Windley, B.F. *et al.* 2009. Paleozoic multiple subduction–accretion processes of the southern Altaiids. *American Journal of Science*, **309**, 221–270, <https://doi.org/10.2475/03.2009.02>
- Xie, W., Luo, Z.-Y., Xu, Y.-G., Chen, Y.-B., Hong, L.-B., Ma, L. and Ma, Q. 2016a. Petrogenesis and geochemistry of the Late Carboniferous rear-arc (or back-arc) pillow basaltic lava in the Bogda Mountains, Chinese North Tianshan. *Lithos*, **244**, 30–42, <https://doi.org/10.1016/j.lithos.2015.11.024>
- Xie, W., Xu, Y.-G., Chen, Y.-B., Luo, Z.-Y., Hong, L.-B., Ma, L. and Liu, H.-Q. 2016b. High-alumina basalts from the Bogda Mountains suggest an arc setting for Chinese Northern Tianshan during the Late Carboniferous. *Lithos*, **256**, 165–181, <https://doi.org/10.1016/j.lithos.2016.04.005>
- Xie, W., Xu, Y.-G., Luo, Z.-Y., Liu, H.-Q., Hong, L.-B. and Ma, L. 2016c. Petrogenesis and geodynamic implications of the Late Carboniferous felsic volcanics in the Bogda belt, Chinese Northern Tianshan. *Gondwana Research*, **39**, 165–179, <https://doi.org/10.1016/j.gr.2016.07.005>
- Xu, X., Chen, C., Ding, T., Liu, Y. and Li, Q. 2008. Discovery of Lisa basalt northwestern edge of Junggar Basin and its geological significance. *Xinjiang Geology*, **26**, 9–16 [in Chinese with English abstract].
- Yang, Y.-T. 2013. An unrecognized major collision of the Okhotomorsk Block with East Asia during the Late Cretaceous, constraints on the plate reorganization of the Northwest Pacific. *Earth-Science Reviews*, **126**, 96–115, <https://doi.org/10.1016/j.earscirev.2013.07.010>
- Yang, Y.-T., Guo, Z.-X., Song, C.-C., Li, X.-B. and He, S. 2015. A short-lived but significant Mongol–Okhotsk collisional orogeny in latest Jurassic–earliest Cretaceous. *Gondwana Research*, **28**, 1096–1116, <https://doi.org/10.1016/j.gr.2014.09.010>
- Yang, Y.-T., Guo, Z.-X. and Luo, Y.-J. 2017. Middle–Late Jurassic tectono-stratigraphic evolution of Central Asia, implications for the collision of the Karakoram–Lhasa Block with Asia. *Earth-Science Reviews*, **166**, 83–110, <https://doi.org/10.1016/j.earscirev.2017.01.005>
- Yin, J., Wang, Y. *et al.* 2023. Episodic long-term exhumation of the Tianshan Orogenic Belt: new insights from multiple low-temperature thermochromometers. *Tectonics*, **42**, <https://doi.org/10.1029/2022tc007469>
- Yu, Y., Sun, M. *et al.* 2017. Whole-rock Nd–Hf isotopic study of I-type and peraluminous granitic rocks from the Chinese Altai: constraints on the nature of the lower crust and tectonic setting. *Gondwana Research*, **47**, 131–141, <https://doi.org/10.1016/j.gr.2016.07.003>
- Yuan, J.-G., Tong, Y., Zhang, H.-F. and Geng, X.-X. 2023. Partial melting of thickened lower crust in the intraplate setting: constraints from triassic posttectonic baishandong granitic pluton in Eastern Tianshan. *International Geology Review*, **65**, 253–277, <https://doi.org/10.1080/00206814.2022.2042861>
- Zhang, Q., Jin, W.J. *et al.* 2006. A model of delamination of continental lower crust. *Acta Petrologica Sinica*, **2**, 265–276 [in Chinese with English abstract].
- Zhang, X., Zhao, G., Sun, M., Han, Y. and Liu, Q. 2017. Triassic magmatic reactivation in Eastern Tianshan, NW China: evidence from geochemistry and zircon U–Pb–Hf isotopes of granites. *Journal of Asian Earth Sciences*, **145**, 446–459, <https://doi.org/10.1016/j.jseas.2017.06.022>
- Zhao, L., Chen, H., Hollings, P. and Han, J. 2019. Tectonic transition in the Aqishan–Yamansu belt, Eastern Tianshan: constraints from the geochronology and geochemistry of Carboniferous and Triassic igneous rocks. *Lithos*, **344**, 247–264, <https://doi.org/10.1016/j.lithos.2019.06.023>
- Zhu, W., Wang, F., Cao, Y. and Wang, S. 2020. Tectono-magmatic events in Tianshan Range and adjacent areas during Yanshanian Movement period. *Acta Geologica Sinica*, **5**, 1331–1346 [in Chinese with English abstract].